Photoinduced Dynamic Gelation and Deformations Based on Molecular Crystal Microrods Stimulated by *Z*-to-*E* Photoisomerization

Yu-Hao Li[1]†, Jiang-Tao Liu[1]†, Ya-Bing Sun[1],Yun-Peng Huang[1], Jia-Wang Hou[1], Yikai Xu[1], Chen-Chen Zhang[1], Tian-Yi Xu[1], Fei Tong[1]*

1. Key Laboratory for Advanced Materials and Joint International Research Laboratory of Precision Chemistry and Molecular Engineering, Feringa Nobel Prize Scientist Joint Research Center, Frontiers Science Center for Materiobiology and Dynamic Chemistry Institute of Fine Chemicals, School of Chemistry and Molecular Engineering, East China University of Science and Technology, 130 Meilong Road, Shanghai, 200237 (China)

E-mail of Corresponding Author:

feitong@ecust.edu.cn,

Experimental Section

All the reagents and solvents employed were commercially available and used as received without further purification. Milli-Q water (18 ΩM/cm) was used throughout the experiments and measurements. All nuclear magnetic resonance (NMR) spectra were measured on a Bruker AV-400 spectrometer, using deuterated acetone-d_6 as solvent at 298K. High-resolution time-of-flight mass spectrometry (HR-MS) was performed using an LCT Premier XE mass spectrometer from the Water Company of the United States. Steady-state absorption and emission spectra were recorded on a Shimadzu RF-6000 spectrophotometer. The optical microscopy measurements were conducted using the Leica DM750 microscope equipped with a QTF500 digital camera. The microscopy fluorescence measurements were performed using a TL-3201LED fluorescence microscope (equipped with a 20MP USB 3.0 digital camera). All powder X-ray diffraction (PXRD) data were collected on an X-ray powder diffractometer (Rigaku, 18 kW/D/Max2550VB/PC, Cu Kα radiation, λ = 1.5418 Å, 40 kV/100 mA power) at room temperature. Single-crystal XRD data were collected on a double target micro focal spot single-crystal X-ray diffraction system (D8 Venture (Mo), Bruker, Germany) at 213 K.

^{1}H NMR Measurements

As for solid-state samples, 5 mg of the crystals were directly irradiated by visible light (450 nm) for different periods. Then, the irradiated samples were dissolved in 0.5 mL of acetone-d_6 for ^{1}H NMR measurements. All NMR tubes were wrapped in aluminum foils during the sample shipping process to eliminate ambient light illumination.

Single Crystal Preparation

1 mmol APA powders were dissolved into 200 μL dry *N, N*-dimethylformamide (DMF) to form a 0.5 M homogenous solution. The solution was placed in an open sample bottle at room temperature. After the solvent was volatilized, single-crystals for structure determination were gathered.

*Synthesis of **APA***

Synthesis of (*Z*)-3-(anthracen-9-yl)-2(pyridin-4-yl)acrylonitrile (**APA**). Specifically, anthracene-9-carboxaldehyde, 4-pyridylacetonitrile (1.5 equivalents), and potassium t-butoxide (2.0 equivalents) were dissolved in ethanol and stirred at 80℃ for 4 hours. Finally, the reaction mixture was cooled to room temperature and the product was filtered and washed with cold methanol and crystallized from $CHCl_3$: methanol (1:3, v/v) solvent to obtain bright yellow powders. (84.5% yield, Fig. S1).^{1}H NMR (400 MHz, Acetone-d_6) δ 9.14 (d, J = 1.0 Hz, 1H), 8.85 – 8.79 (m, 2H), 8.74 (s, 1H), 8.23 – 8.13 (m, 4H), 7.99 – 7.93 (m, 2H), 7.65 – 7.54 (m, 4H) (Fig. S2). ^{13}C NMR (101 MHz, Acetone-d_6) δ 151.82, 145.84, 141.39, 132.33, 130.23, 130.17, 130.00, 128.80, 127.86, 126.69, 126.14, 121.22, 120.29, 116.44 (Fig. S3). HR-MS(EI): calculated for $C_{22}H_{14}N_2$, $[M+H]^+$ =307.1200, found =306.1160 (Fig. S4).

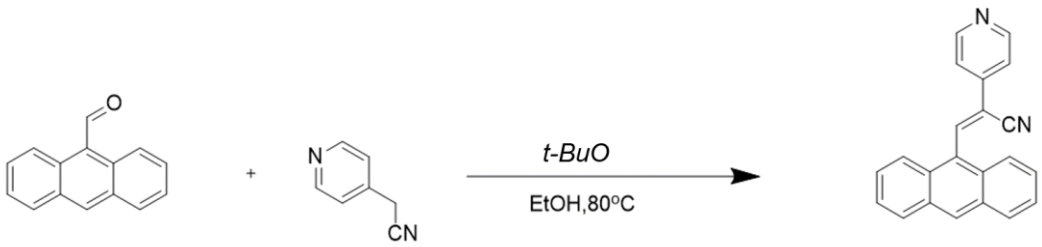

Fig. S1. Synthetic procedure of compound **APA**

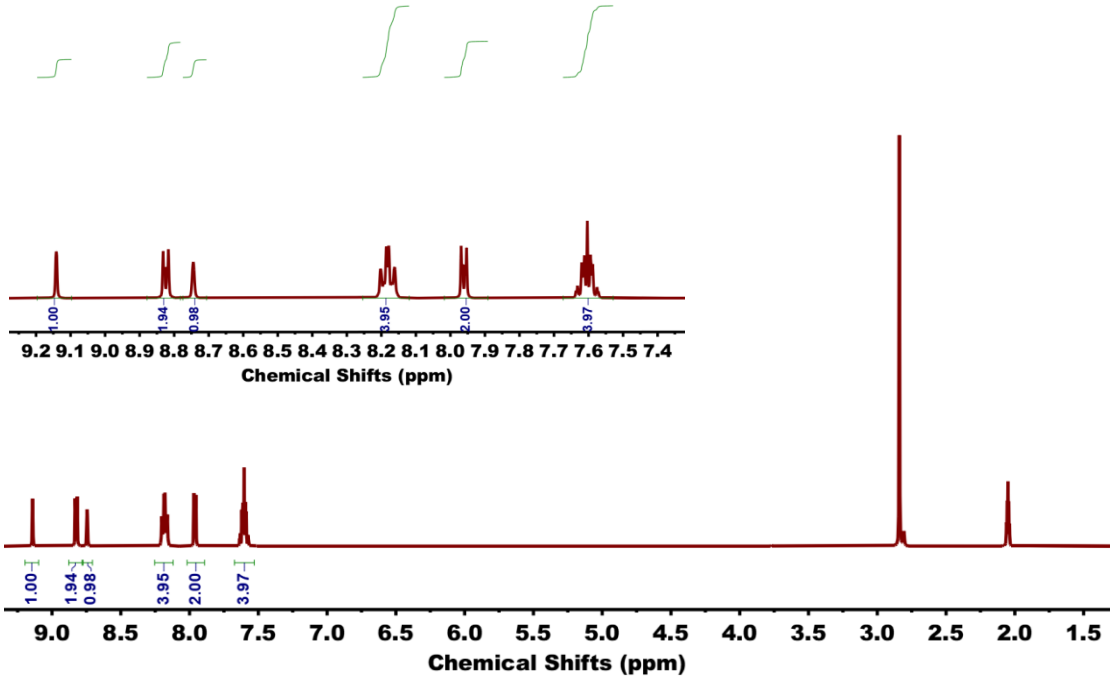

Figure S2. In the ^{1}H NMR spectra of **APA**, acetone-d_6 was used as a solvent. On the spectrum, the multiple peak at 2.05 ppm is attributed to the solvent peak, while the single peak at 2.85 ppm is attributed to the water signal. In addition, spectra ranging from 7.30 ppm to 9.10 ppm were used for insertion analysis.

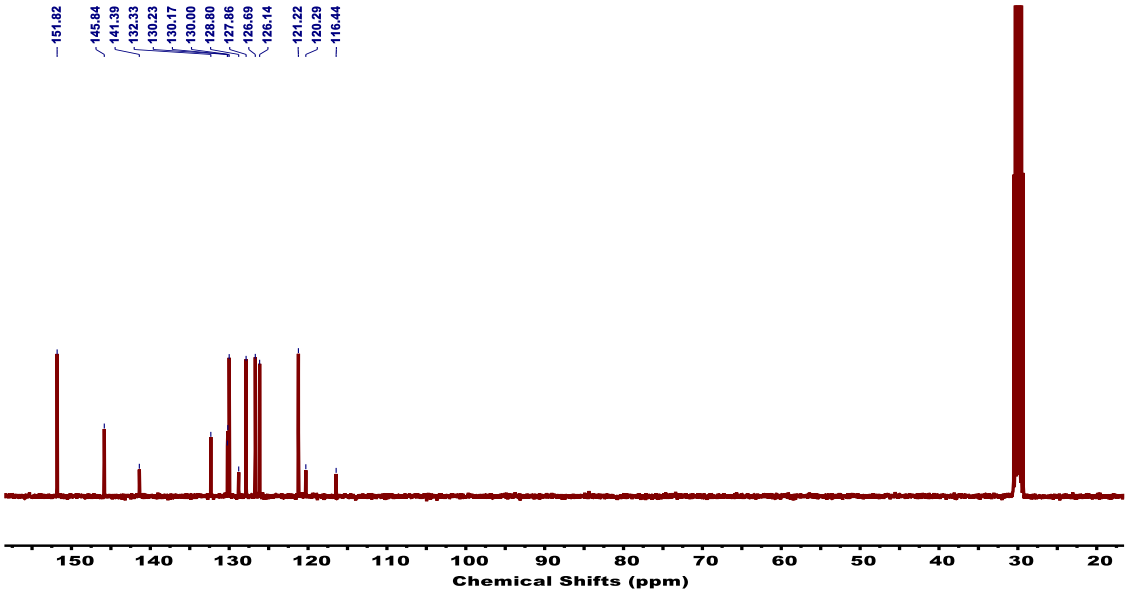

Fig. S3. The ^{13}C NMR spectra of **APA**, acetone-d_6 was used as a solvent. the multiple peak at 28.85 ppm is attributed to the solvent peak.

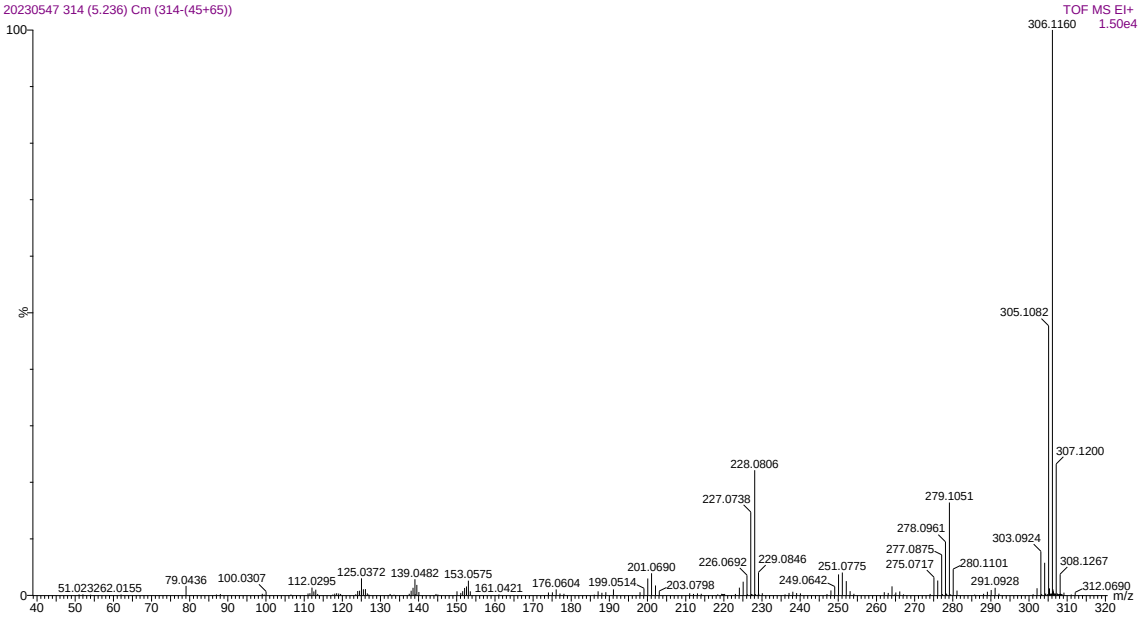

Fig. S4. The HR-MS (EI) spectra of **APA**.

Table S1. Crystal data and structure refinement for **APA**.

Identification code	d8v23273	
Empirical formula	C22 H14 N2	
Formula weight	306.35	
Temperature	213(2) K	
Wavelength	0.71073 Å	
Crystal system	Orthorhombic	
Space group	*P b c a*	
Unit cell dimensions	a = 14.0461(5) Å	α= 90°.
	b = 12.8296(4) Å	β= 90°.
	c = 17.1929(6) Å	γ = 90°.
Volume	3098.26(18) $Å^3$	
Z	8	
Density (calculated)	1.314 Mg/m^3	
Absorption coefficient	0.078 mm^{-1}	
F(000)	1280	
Crystal size	0.170 x 0.150 x 0.120 mm^3	
Theta range for data collection	2.900 to 25.996°.	
Index ranges	-17<=h<=16, -15<=k<=14, -21<=l<=21	
Reflections collected	20335	
Independent reflections	3043 [R(int) = 0.0817]	
Completeness to theta = 25.242°	99.8 %	
Absorption correction	Semi-empirical from equivalents	
Max. and min. transmission	0.7456 and 0.5914	
Refinement method	Full-matrix least-squares on F^2	
Data / restraints / parameters	3043 / 0 / 217	
Goodness-of-fit on F^2	1.081	
Final R indices [I>2sigma(I)]	R1 = 0.0536, wR2 = 0.0992	
R indices (all data)	R1 = 0.0910, wR2 = 0.1156	
Extinction coefficient	n/a	
Largest diff. peak and hole	0.198 and -0.192 $e.Å^{-3}$	

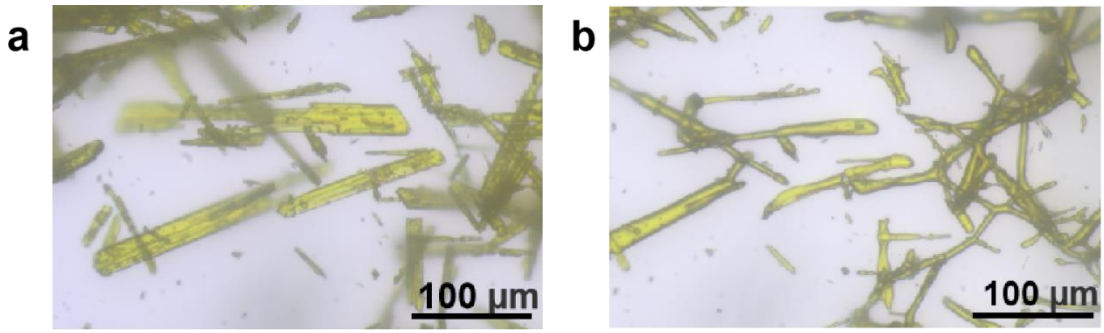

Fig. S5. Optical microscope images of bulk crystals of **APA** molecules (a) before and (b) after light irradiation (450 nm).

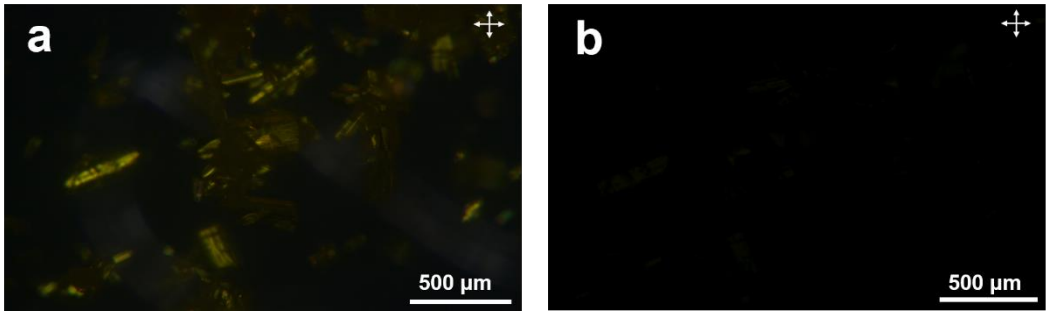

Fig. S6. (a) Cross-polarized microscope images of bulk crystals of **APA** molecules (a) before and (b) after light irradiation.

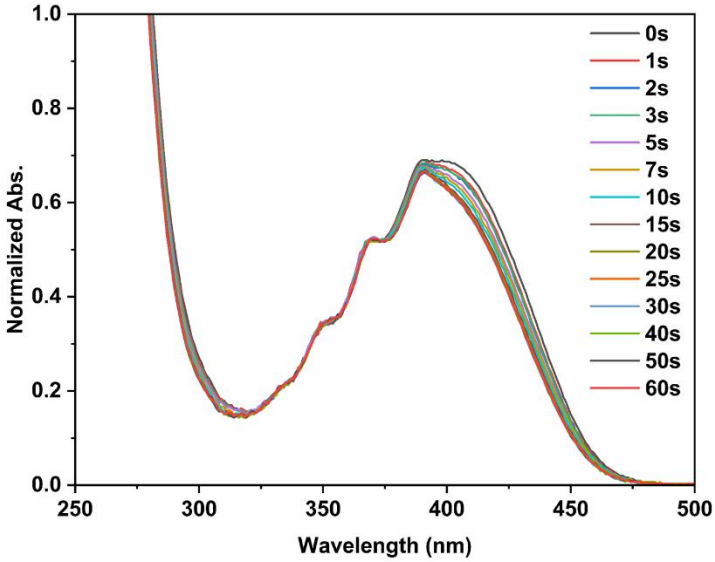

Fig. S7. UV-vis absorption spectra of **APA** in THF solution ([**APA**] ~ 1.0×10^{-5}M) with irradiation at different periods.

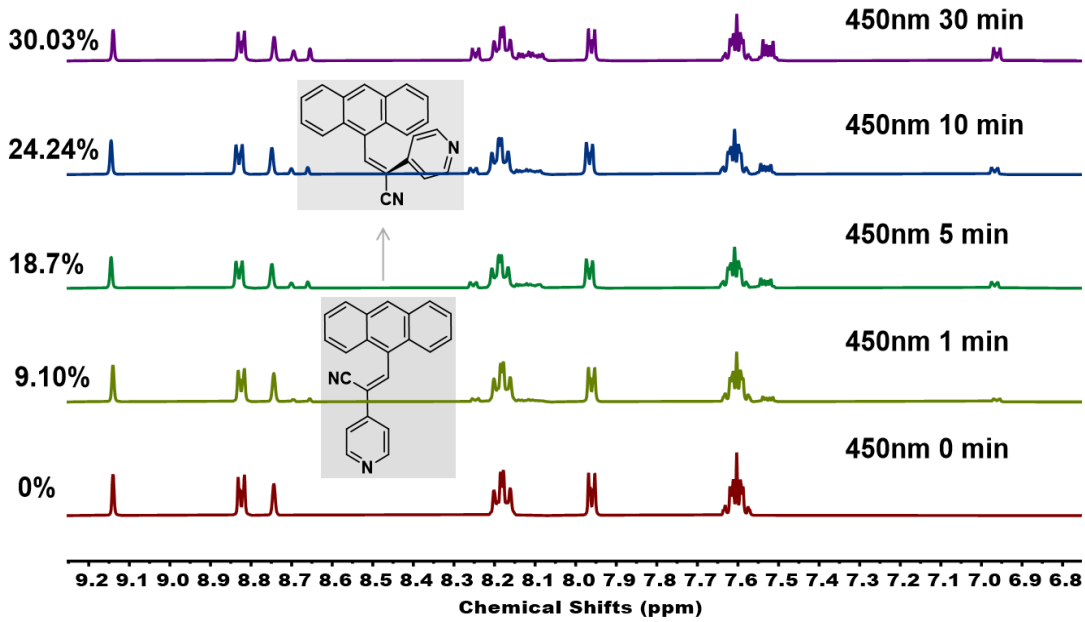

Fig. S8. [1]H NMR spectra of the **APA** polycrystals with different periods of light irradiation.

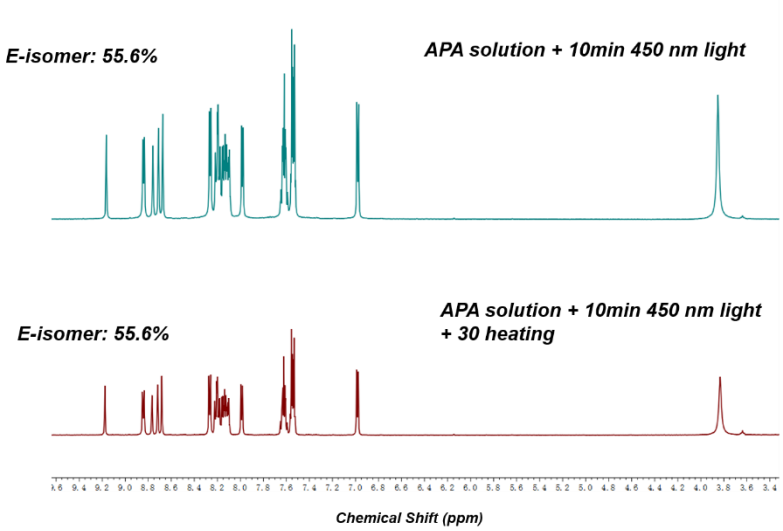

Fig. S9. [1]H NMR spectra of photoreacted **APA** solution samples irradiated with 450 nm light and upon heating, showing no reversion (acetone-d_6 as solvent).

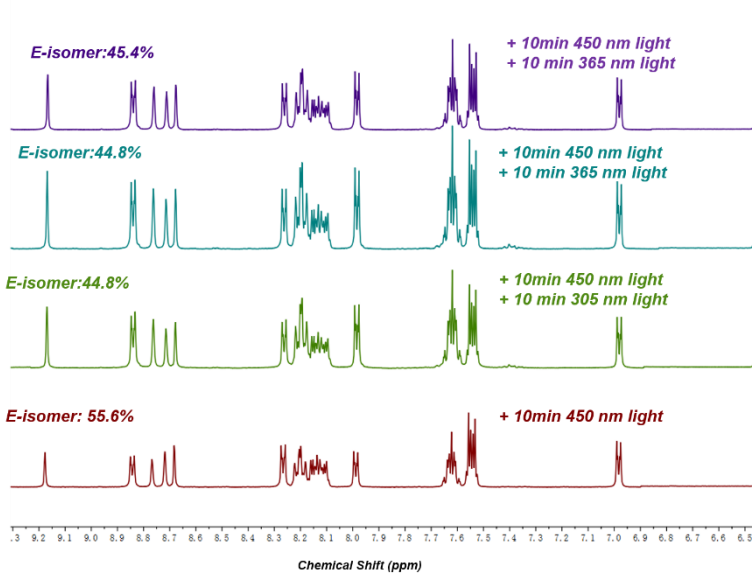

Fig. S10. ^{1}H NMR spectra of photoreacted **APA** solution samples irradiated with 450 nm light and following irradiation of shorter wavelength light, showing partial reversion (acetone-d_6 as solvent).

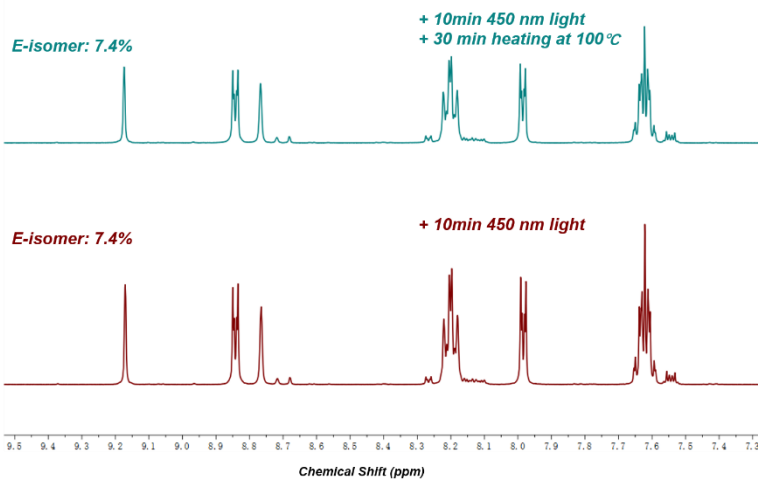

Fig. S11. ^{1}H NMR spectra of photoreacted **APA** polycrystals irradiated with 450 nm light and upon heating, showing no revision. **APA** solids were dissolved in acetone-d_6 after light irradiation or heating for NMR measurements.

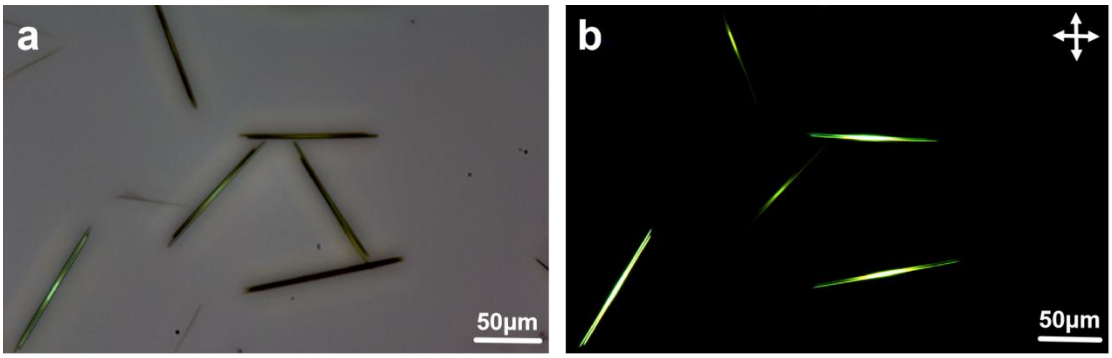

Fig. 12. The optical microscope and cross-polarized microscope images of the prepared **APA** microrods in the aqueous surfactant solution. Scale bars: 50 μm.

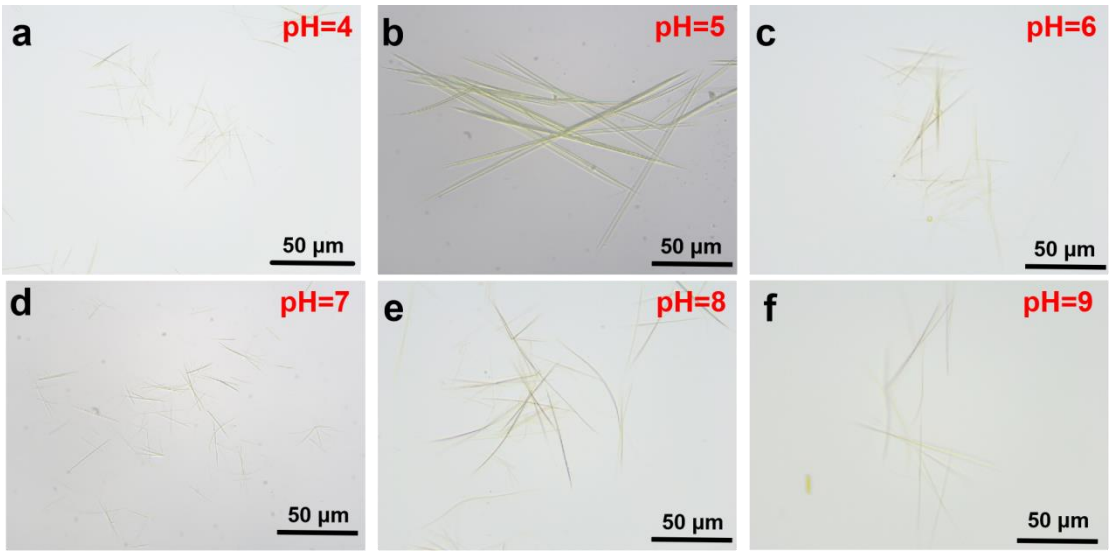

Fig. S13. (a)-(f) Optical microscope images of the **APA** microrods grown under different pH conditions. Scale bars: 50 μm.

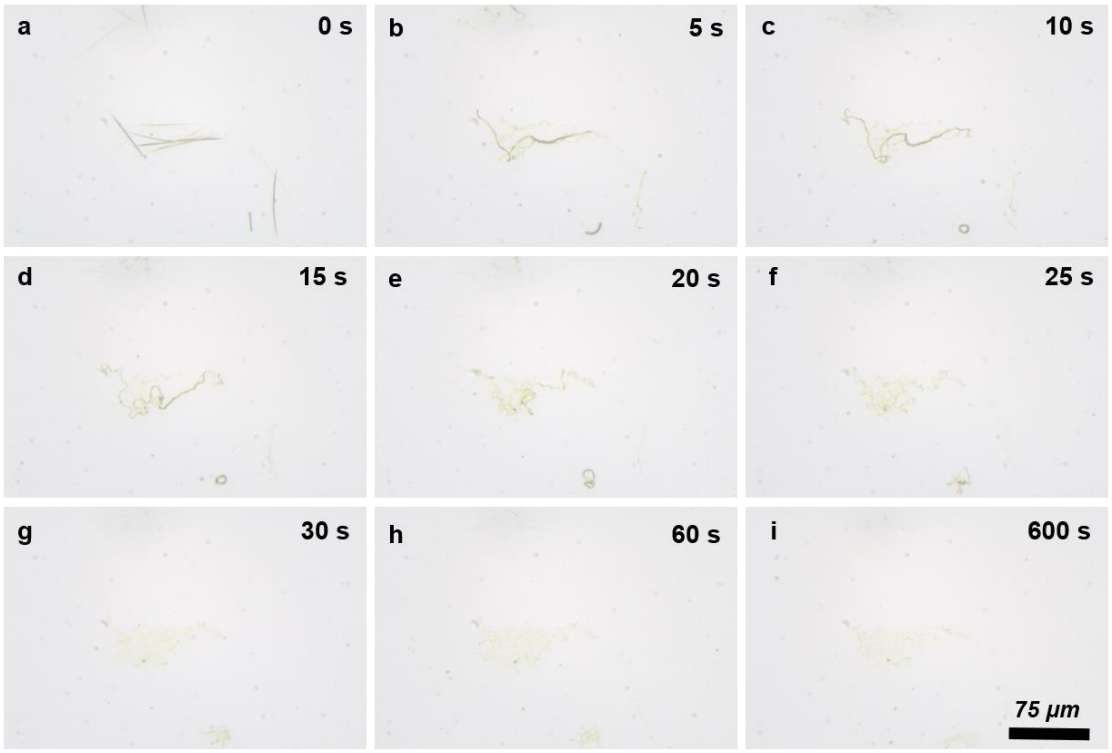

Fig. S14. Sequential optical microscope images of **APA** microrods in the aqueous surfactant solution under visible light irradiation.

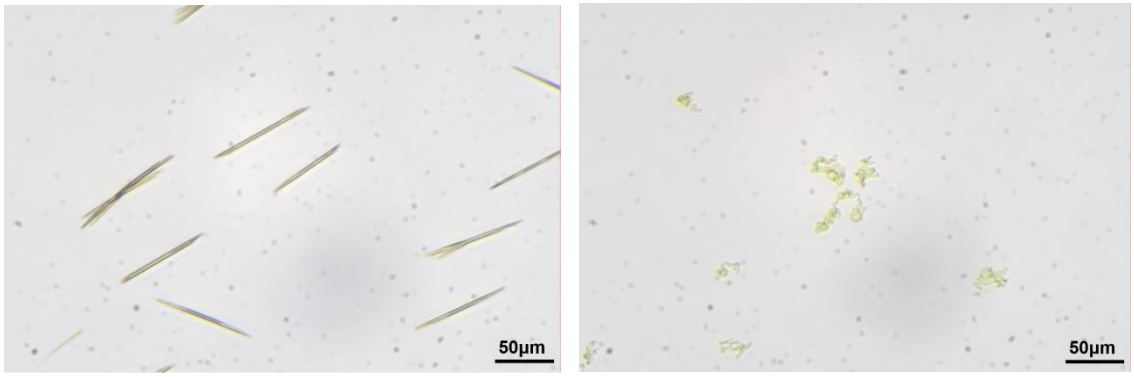

Fig. S15. Optical microscope images of **APA** microrods in the aqueous surfactant solution (a) before and (b) after light irradiation. The **APA** microrods suggest vigorous photoresponsive properties. Scale bars: 50 μm.

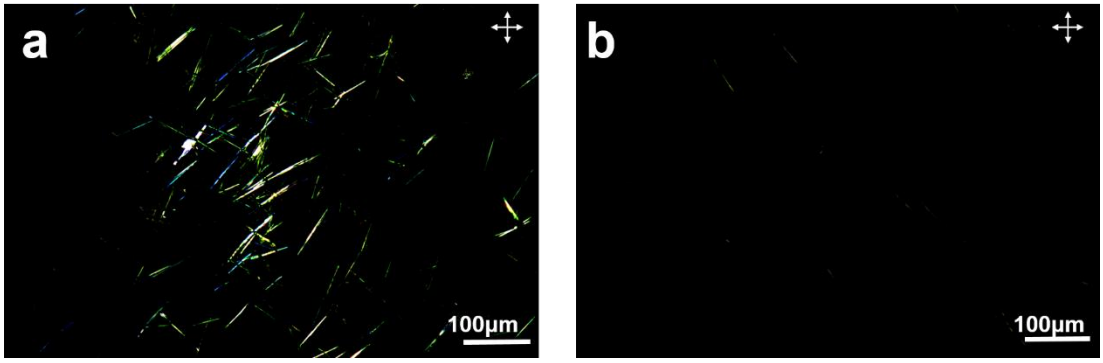

Fig. S16. (a) Cross-polarized microscope images of **APA** microrods in the aqueous surfactant solution (a) before and (b) after light irradiation.

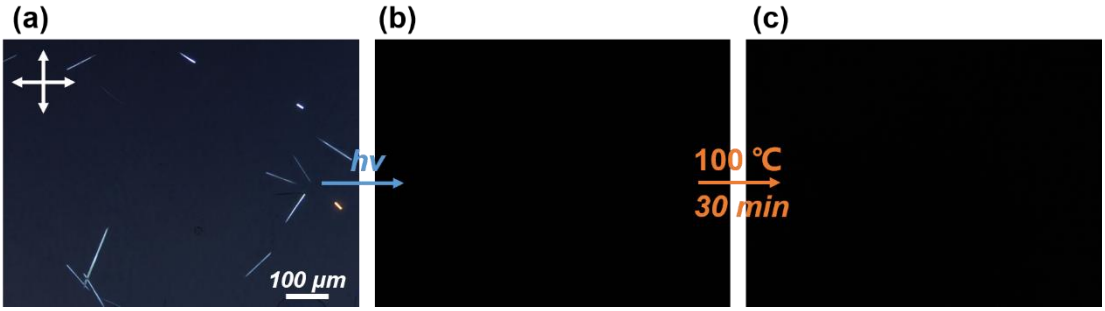

Fig. S17. (a) The cross-polarized microscope image of the **APA** microrods in the aqueous surfactant solution before light irradiation. (b) The cross-polarized microscope image of the **APA** microrods in the aqueous surfactant solution after light irradiation. (c) Cross-polarized microscope image of the photoreacted **APA** microrods after heating at 100℃ for 30 min, showing no recrystallization.

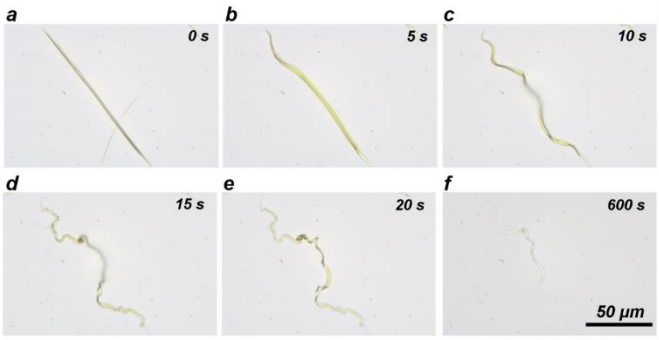

Figure No.	Pixel Value	Expansion Ratio
a	332.339	
b	349.626	5.2%
c	392.514	18.1%
d	508.266	52.9%
e	534.716	60.9%

Fig. S18. Estimating the length expansion during light irradiation by counting the pixels in an **APA** microrod.

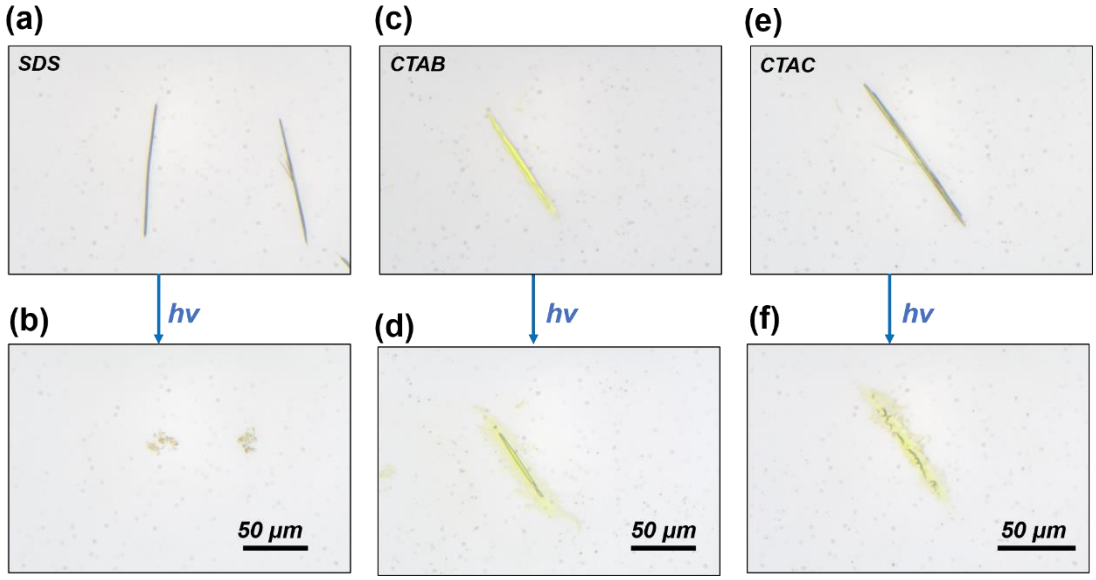

Fig. S19. (a)-(b) Optical microscope images of **APA** microrods in the SDS solution before and after light irradiation. (c)-(d) Optical microscope images of an **APA** microrod in the CTAB solution before and after light irradiation. (e)-(f) Optical microscope images of an **APA** microrod in the CTAC solution before and after light irradiation.

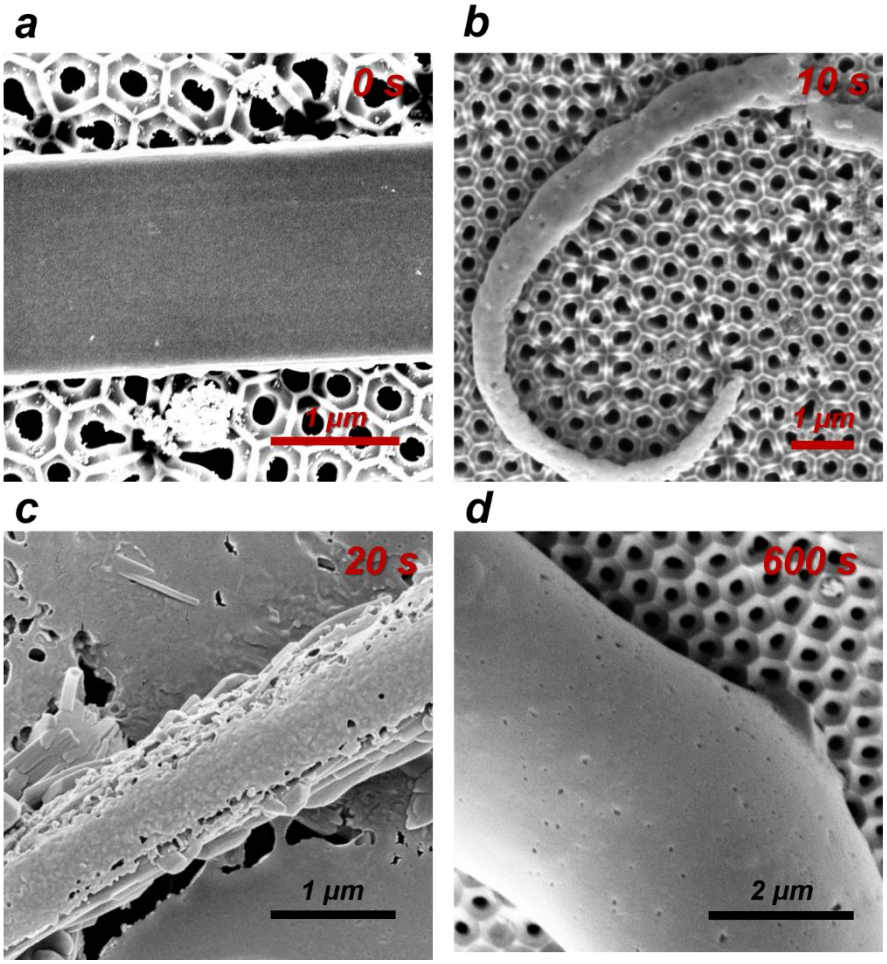

Fig. S20. The SEM images of the **APA** microrods exhibits crystal-to-gel transformation upon visible light irradiation. The upright time indicates the illumination periods.

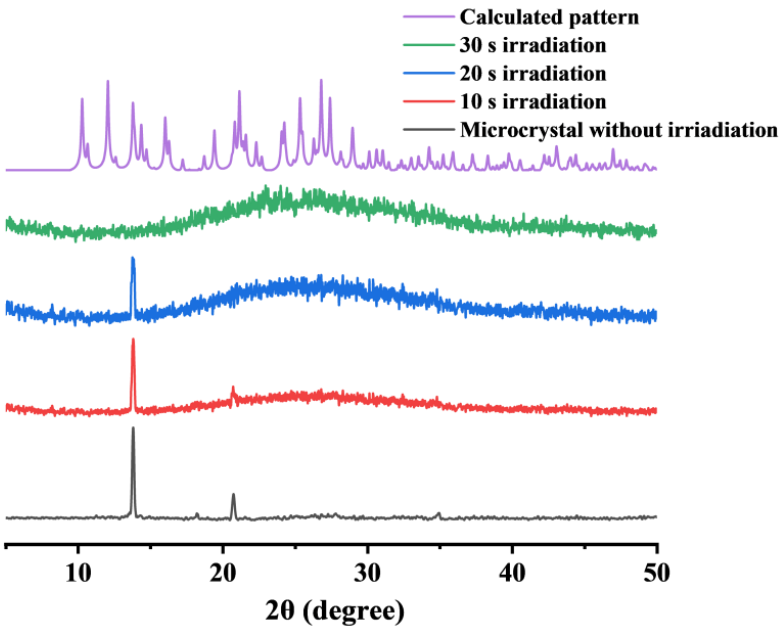

Fig. S21. Powder X-ray diffraction (PXRD) patterns of **APA** microrods after being filtered, rinsed, and placed on the AAO template surface under varying irradiation durations, showing the crystal-to-amorphous upon light irradiation.

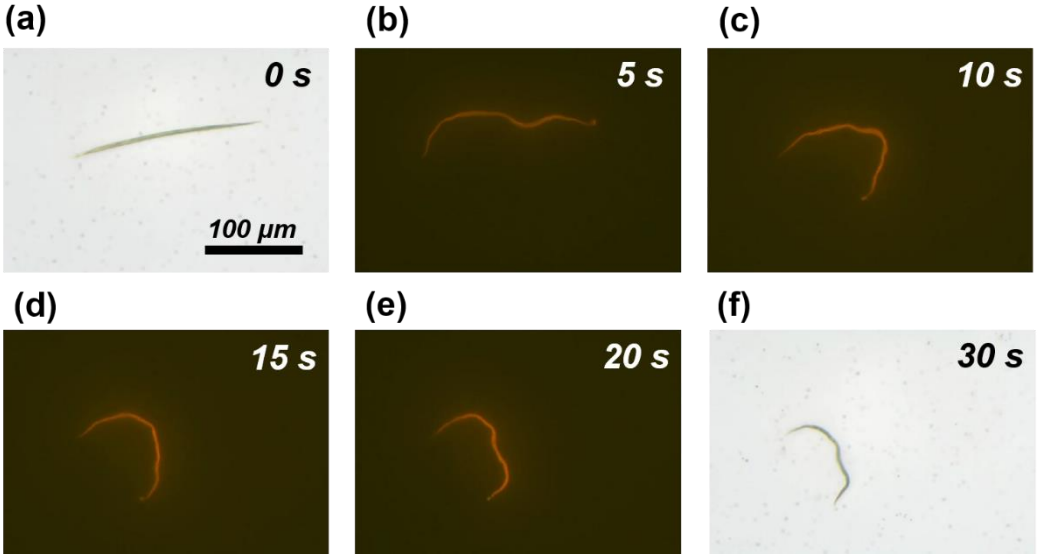

Fig. S22. Sequential optical microscope images of an **APA** microrod in pure water under light irradiation. The time indicates the duration of light irradiation.

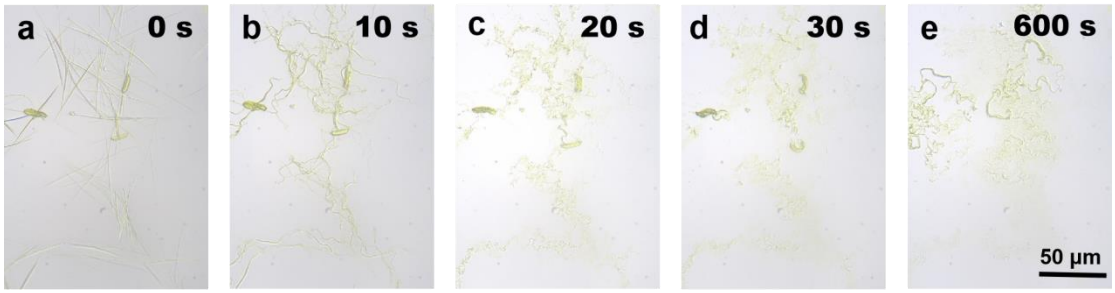

Fig. S23. (a)-(e) Sequential optical microscope images of the **APA** microrods in the aqueous surfactant solution exhibiting crystal-to-gel transformation upon visible light irradiation. The upright time indicates the illumination periods. Scale bars: 50 μm.

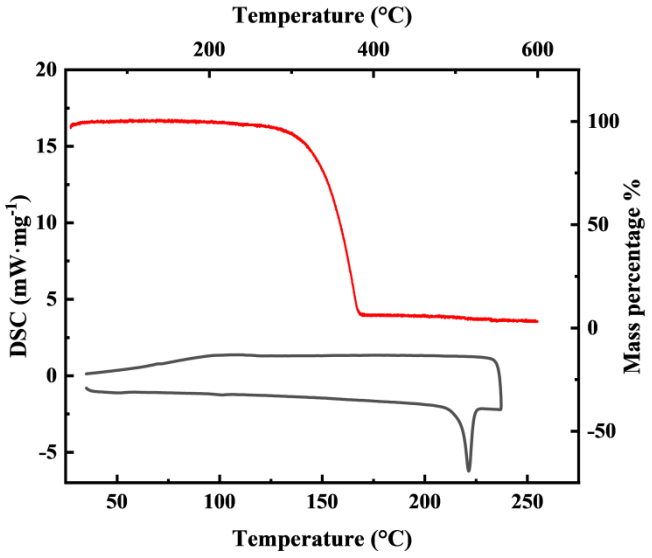

Fig. S24. DSC curves and TGA curves of **APA** crystals.

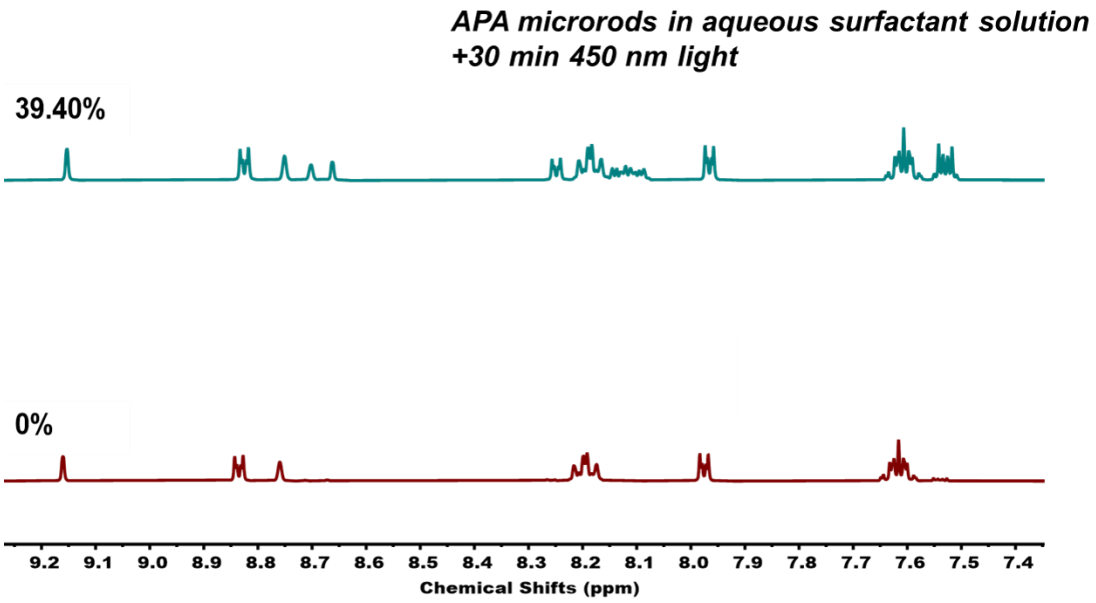

Fig. S25. ^{1}H NMR of **APA** microrods in the aqueous surfactant solution under 450 nm light for 30 min, generating 39.4% *E*-isomer. The product was filtered, rinsed with water, dried before being dissolved in the deuterated solvent.

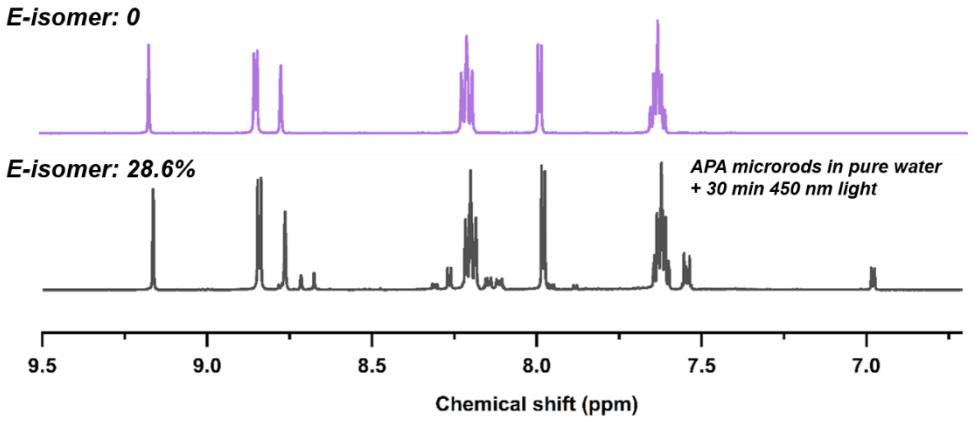

Fig. S26. ^{1}H NMR spectra of **APA** microrods in pure water under light irradiation for 30 min. The product was filtered and dried before being dissolved into acetone-d_6.

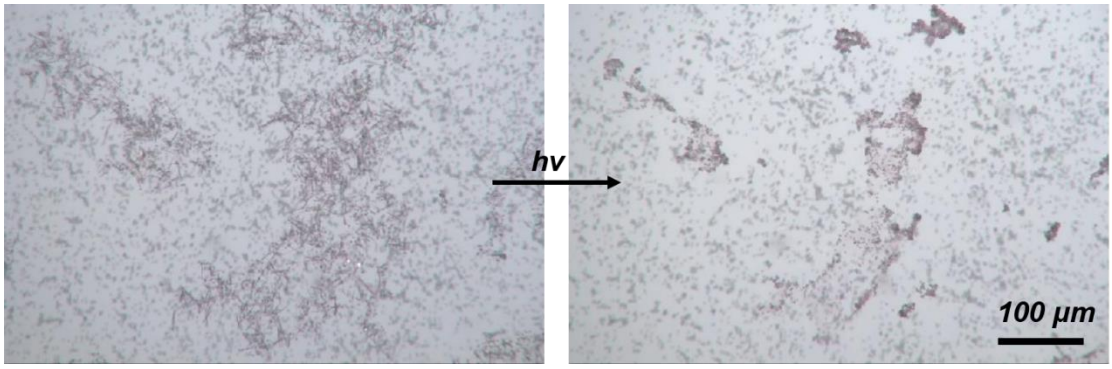

Fig. S27. Optical microscope images of silica microspheres collected and gathered by **APA** microrods in the aqueous surfactant solution under 450 nm irradiation. Scale bars: 100 μm.

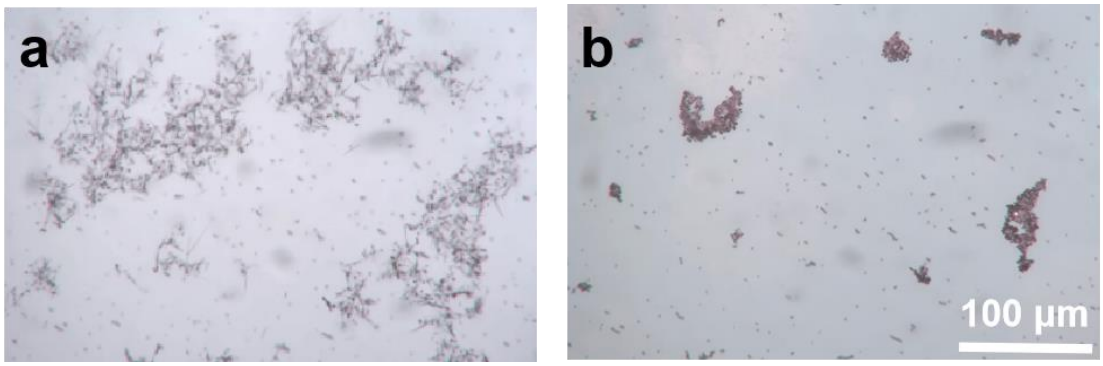

Fig. S28. Optical microscope images of Fe_3O_4 microspheres collected and gathered by **APA** microrods in the aqueous surfactant solution under 450 nm irradiation. Scale bars: 100 μm.

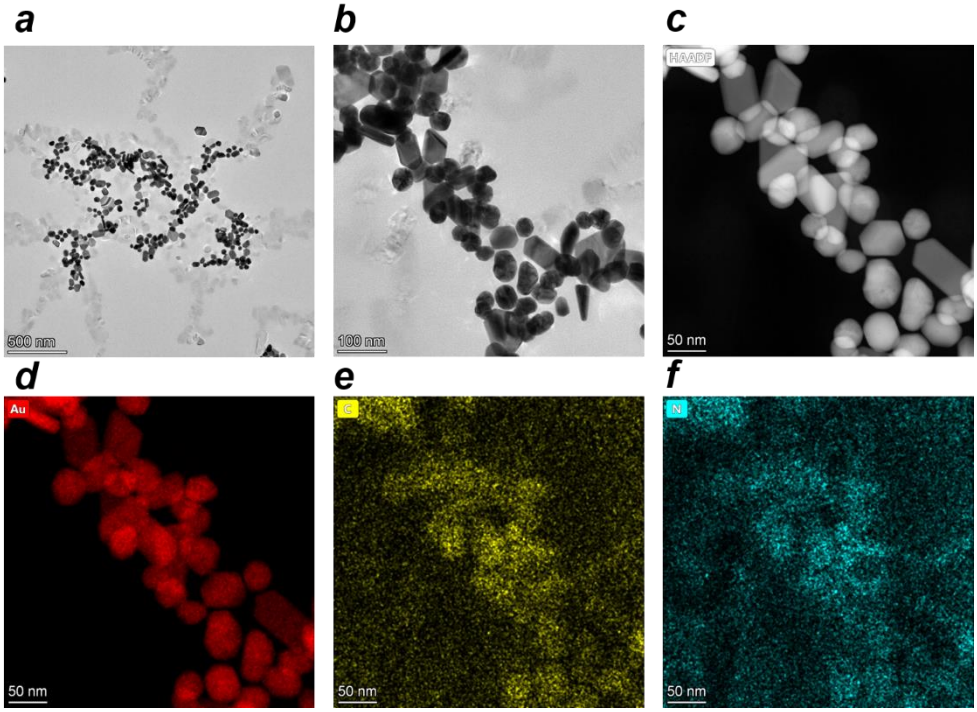

Fig. S29. (a) The TEM image of Au nanoparticles incorporated inside the **APA** gels after light irradiation. (b) The magnified TEM image of Au nanoparticles inside the **APA** gels. (c) The HAADF and EDS mapping images of Au nanoparticles inside the **APA** gels.

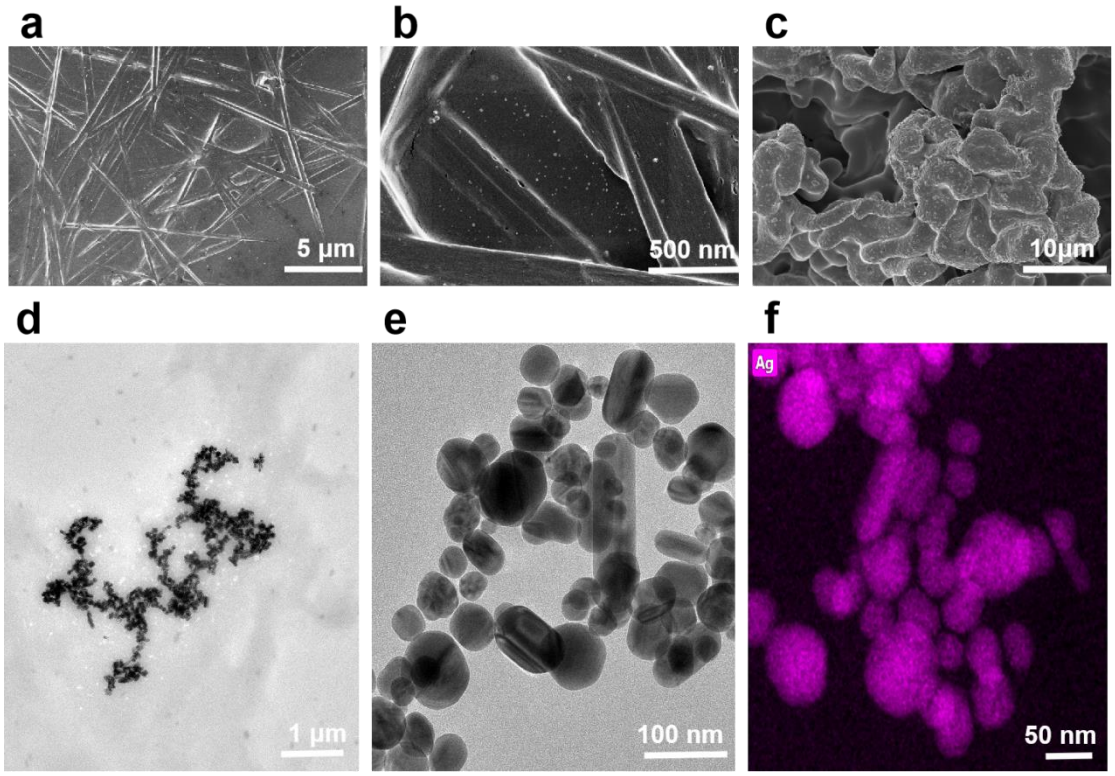

Fig. S30. (a)-(c) SEM images of Ag nanoparticles that adhere and are engulfed inside the light-irradiated APA gels. (d)-(e) TEM images of Ag nanoparticles that are incorporated inside the APA gels. (f) High-resolution TEM image with element analysis showing Ag nanoparticles engulfed inside the APA gels.

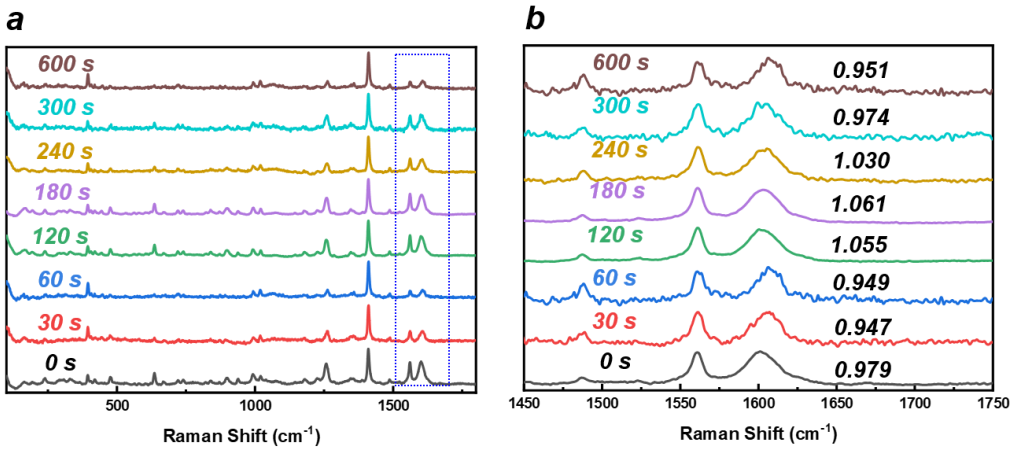

Fig. S31. (a) Raman spectra of pristine **APA** microrods in the aqueous surfactant solution under 450 nm under the light irradiation of varying durations. (b) Enlarged spectra of the 1450-1750 cm^{-1} region, with the percentage indicating the peak intensity ratio between 1560 cm^{-1} and 1607 cm^{-1}.

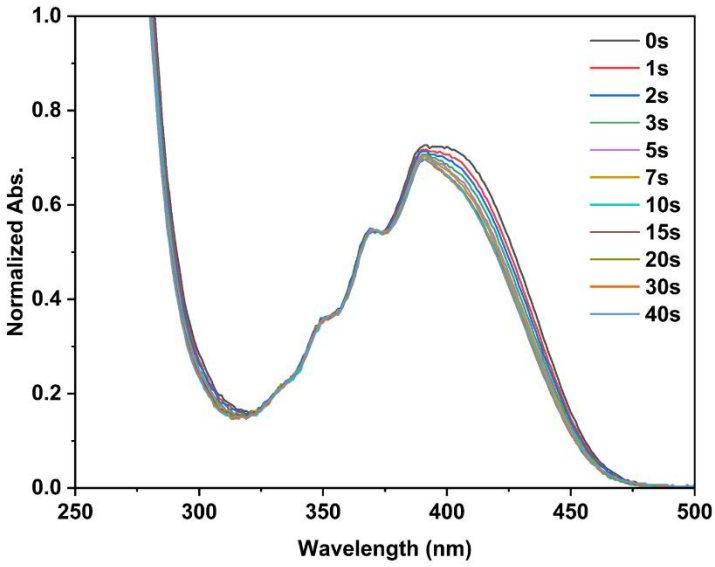

Fig. S32. UV-vis absorption spectra of Ag-**APA** system ([**APA**] ~ 1.0×10^{-5} M, [Ag nanoparticles]~3.0×10^{12} cm^{-1}, THF as solvent) with varied irradiation durations.

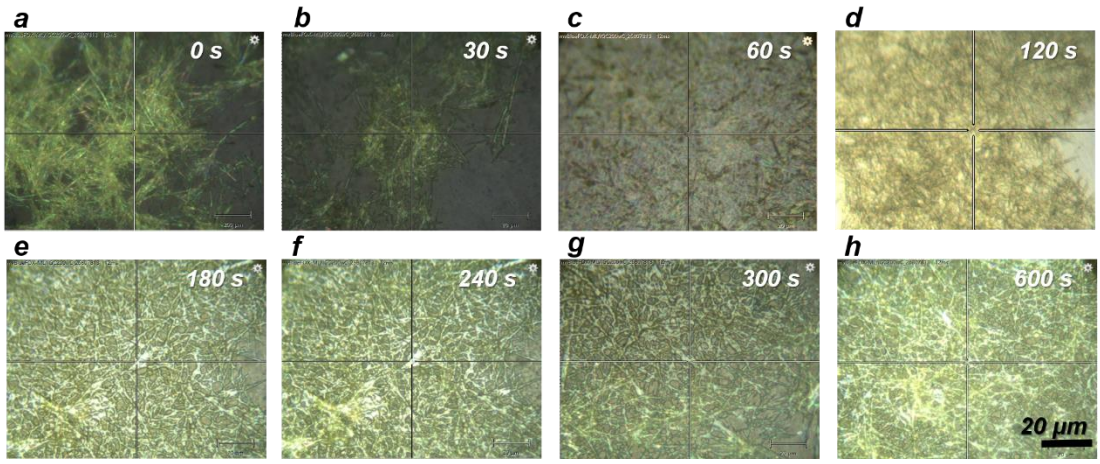

Fig. S33. (a)-(h) Sequential microscope images of **APA** microrods with Ag nanoparticles in the aqueous surfactant solution under visible light irradiation with varying irradiation durations.

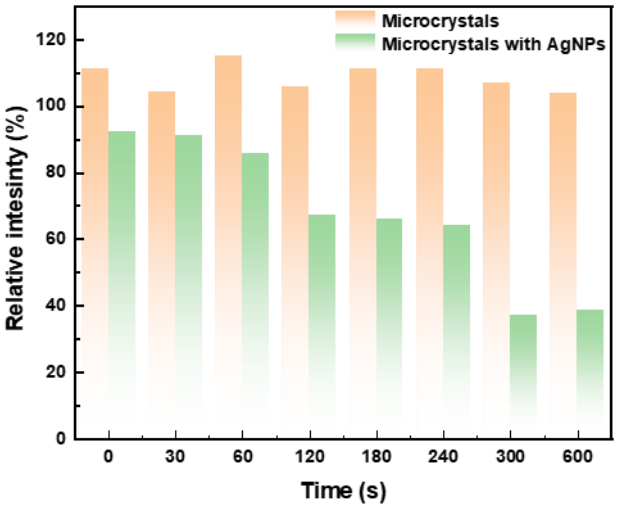

Fig. S34. Comparison of the percentage indicating the peak intensity ratios between 1560 cm^{-1} and 1607 cm^{-1} of pristine **APA** microrods and **APA** microrods with Ag nanoparticles with different light irradiation.